Design and Analysis of Ring-Focus Reflector Antenna using Method of Moments Solution of Electric Field Integral Equation

I. Ismatullah [1], Ghulam Ahmad [1,2], and Shafaat A. K. M. Ali [1]

[1] Geo-Sat Payload Division
Satellite Research and Development Center, Lahore/Karachi, 54000, Pakistan
ismatullah@gmail.com

[2] Faculty of Engineering and Physical Sciences
University of Surrey, Guildford, GU2 7XH, United Kingdom
g.ahmad@surrey.ac.uk

Abstract ─ Ring-focus dual reflector antennas have been employed in various satellite communication applications because of their higher gain and geometrical compactness as compared to the conventional Cassegrain or Gregorian counterparts. In this contribution the geometrical design, full-wave analysis and testing of a ring-focus dual reflector antenna based on axially displaced ellipse (ADE) configuration are reported. The geometrical design of this dual reflector system is conceived through conic section formulations. An analytical methodology based on multilevel fast multipole method (MLFMM) accelerated method of moments (MoM) solution of surface integral equations for open perfect electrically conducting objects was developed for its RF performance prediction. The distinctive nature of surface current distributions of a ring-focus subreflector is investigated and compared with that of a Cassegrain counterpart. Finally, the developed procedure was applied to predict the performance of a 35 wavelength ADE ring focus antenna. A close agreement of predicted and measured performance was observed which proves the validity of our fast analytical procedure.

Index Terms ─ Axially displaced ellipse, EFIE, MLFMM, MoM, ring focus antenna, SATCOM.

I. INTRODUCTION

Design methods for efficiency enhancement and sidelobes reduction in high gain antennas have always been a topic of keen interest among antenna design engineers. Increasing the gain of a communication antenna directly increases signal to noise ratio and hence the communication link can support increased data rates [1]. However, since the antenna gain is proportional to its effective area [2]; the trend towards compactness may pose conflicting requirements. Consequently, the demand for compact yet efficient aperture antennas is on the rise.

A ring-focus reflector antenna is an excellent candidate for high gain compact antennas. It has proved its effectiveness in recent years particularly in SATCOM on the move applications [1,3,4]. A ring focus subreflector can be made several times smaller in comparison to that of classical Cassegrain/Gregorian antennas. Similarly, the feed horn can be placed closer to a ring focus subreflector without experiencing detrimental blockage effects [1]. The aperture efficiency of a ring-focus antenna can exceed 80% due to its ray inversion features [5,6]. In other reflector antenna configurations the aperture efficiency is relatively less than that of a ring focus design. Although, there exist few exotic designs, e.g., top hat fed reflector antennas [7,8] which can achieve a comparable efficiency. However, it takes significant efforts to meet such a target. In such designs the antenna bandwidth and its cross polarization discrimination (XPD) become potential design concerns.

The geometrical design of a ring-focus reflector antenna can be accomplished by using the necessary design equations for a given set of known parameters and can be found in literature [6,9,10]. However, in the work presented here, a more fundamental approach has been adopted to enable a better design insight and its direct implementation in the GiD pre and postprocessor software [11]. In this approach, primary conic section definitions have been used to obtain the profiles of main- and sub-reflectors. A macro was written to get the complete surface model of a ring-focus reflector in a single run.

When the multilevel fast multipole method (MLFMM) accelerated method of moments (MoM) solution of electric field integral equations (EFIE) [12-19] is solved through an efficient MoM direct method [20], the resulting solution is computationally efficient. Our developed EM solver combines the above two methods to achieve a computationally faster solution of the presented ring focus antenna. This EM solver takes as input the surface mesh which can be generated in GiD

Submitted On: March 4, 2016
Accepted On: January 3, 2018

software. Using our EM solver we investigated the distinctive nature of the surface current density on the presented ring-focus subreflector for its effects on the overall radiation performance.

In Section II the geometrical design of a ring-focus reflector from the basic conic section formulations is presented. Section III provides an overview of the formulation followed in the full-wave analysis of the designed reflector antenna. The developed EM solver was used to predict the performance of a 35 wavelength diameter ring focus antenna which is compared with the measured radiation patterns in Section IV. Section V concludes the work being presented in this paper.

II. GEOMETRICAL DESIGN OF A RING-FOCUS REFLECTOR

A ring-focus dual reflector antenna system based on axially displaced ellipse (ADE) configuration [5,10] is shown in Fig. 1. Due to geometrical optics (GO) an axial ray originating from the feed horn travels towards the main reflector's outer rim after a reflection from a ring focus subreflector. Whereas a ray arriving at subreflector's outer rim travels towards the central portion of the main reflector which is contrary to classical Cassegrain/Gregorian designs. This is known as the ray inversion phenomena of a ring-focus antenna. The whole geometry presented in Fig. 1 is rotationally symmetric about the axis of symmetry (z-axis here). Geometries of main and sub-reflectors can be generated by using the following mathematical treatment.

It is usual to start the antenna design by knowing certain parameters [10]. The gain requirement of an antenna determines its aperture, where the diameter of a subreflector is selected a few percentage of the main reflector's diameter. Focal length is mainly decided by the accommodation space available for the antenna, although longer focal lengths lead to a better XPD. In the work presented here, it is assumed that the diameter of main reflector (D_m), diameter of subreflector (D_s), focal length of the main reflector (F_m) and the location of feed phase center (F_S) as shown in Fig. 1 are already known. It is to be noted that an elliptical subreflector possesses two foci. One of these coincides with the main reflector's focal point. Whereas the second focus is made coincident with the feed phase center for an optimum performance. In the equations given below, P_s (say) represents a point on the main/subreflector and (x_{P_S}, z_{P_S}) represent it's x and z coordinates respectively.

The profile of a parabolic main reflector can be generated by the basic equation of a conic section:

$$z = \frac{\left(x - {}^{D_S}/_{2}\right)^2}{4F_m}, \quad \frac{D_s}{2} \le x \le \frac{D_m}{2}. \tag{1}$$

Keeping in view the ray inversion phenomenon, where ray $\overrightarrow{F_{S1}S_1}$ will travel along $\overrightarrow{S_1F_{S2}M_2}$ after reflection at S_1, the point S_1 can be determined from equation of a straight line. Thus, knowing $x_{S1} = 0$; the z-coordinate of S_1 can be written as:

$$z_{S1} = z_{F_{S2}} + \frac{z_{M2} - z_{F_{S2}}}{x_{M2} - x_{F_{S2}}}\left(x_{S1} - x_{F_{S2}}\right). \tag{2}$$

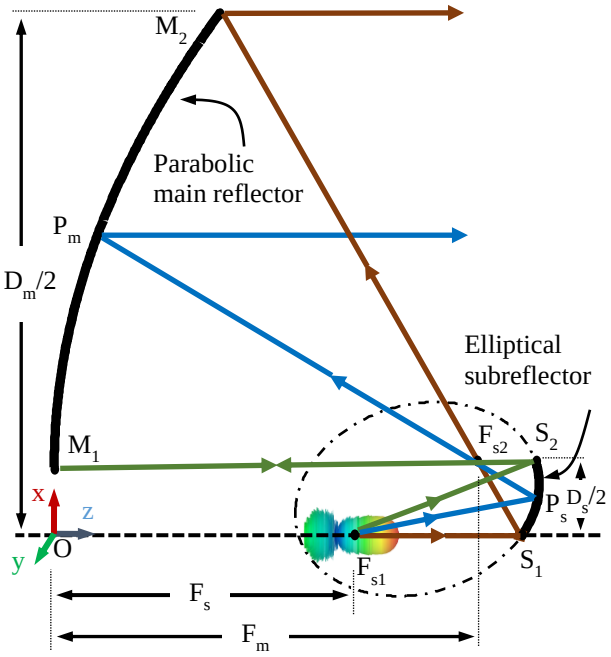

Fig. 1. Geometry of a ring-focus dual reflector antenna.

The semi-major axis "a" of an ellipse can be calculated from its basic property:

$$a = \frac{|\overline{F_{s1}S_1}| + |\overline{F_{s2}S_1}|}{2}. \tag{3}$$

Once "a" is determined, the set of points representing a subreflector can be constructed using quadratic equation's solution of an ellipse:

$$|\overline{F_{s1}P_s}| + |\overline{F_{s2}P_s}| = 2a \; 0 \le x_{P_S} \le \frac{D_s}{2}. \tag{4}$$

Therefore, the solution of (4) for z_{P_S} can be expressed as:

$$z_{P_S} = \frac{-\beta \pm \sqrt{\beta^2 - 4\alpha\gamma}}{2\alpha}, \tag{5}$$

where

$$\alpha = 4\left[(2a)^2 - \left(z_{F_{S2}} - z_{F_{S1}}\right)^2\right], \tag{5a}$$

$$\beta = 4\left[\delta\left(z_{F_{S2}} - z_{F_{S1}}\right) - 8a^2 z_{F_{S2}}\right], \tag{5b}$$

$$\gamma = 16a^2\left[\left(z_{F_{s2}}\right)^2 + \left(x_{P_S} - x_{F_{s2}}\right)^2\right] - \delta^2, \tag{5c}$$

where $\delta = 4a^2 + \left(z_{F_{S2}}\right)^2 - \left(z_{F_{S1}}\right)^2 + \left(x_{P_S} - x_{F_{S2}}\right)^2 - \left(x_{P_S} - x_{F_{S1}}\right)^2$. (5d)

Corresponding to each x_{P_S}, Equation (5) generates two values of z_{P_S}, and ADE geometry can be obtained by using positive discriminant in Equation (5) which corresponds to right-sided (solid) curve of the ellipse as

shown in Fig. 1. Once the 2-dimensional profiles of main and sub-reflectors are obtained, the 3D surface model can be obtained by rotating these profiles around the z-coordinate (see Fig. 1). The locus of the main reflector's focal point (and its coincident subreflector focal point) traces a ring in 3D due to this rotation and hence the name ring-focus.

III. ANALYSIS OF RING-FOCUS REFLECTOR ANTENNA USING MLFMM ACCELARATED MOM SOLUTION OF EFIE

The MoM solution of surface integral equations is a well-known powerful numerical tool for solving electromagnetic problems [12-13]. For the analysis of our ring-focus reflector antenna, electric field integral equations (EFIE) which couples the incident electric field to induced current density on an arbitrary shaped surface has been taken into consideration. In this formulation, the surface S of the ring-focus reflector antenna is replaced by equivalent surface electric current density $\overrightarrow{J_S}$ which radiates the electric and magnetic fields $(\vec{E}, \vec{H})$ in free space. $\overrightarrow{J_S}$ can be obtained by solving [12-16]:

$$\hat{n} \times \left[\hat{n} \times \left\{\iint_S \left[\bar{\bar{G}}_J^E(\vec{r},\vec{r}').\vec{J}_S(\vec{r}')\right]ds' + \vec{E}^{inc}(\vec{r})\right\}\right] = 0, \quad (6)$$

where $\vec{E}^{inc}(\vec{r})$ is the incident electric field, $\hat{n}$ is the outward directed unit surface normal and $\bar{\bar{G}}_J^E(\vec{r},\vec{r}')$ represents the free space dyadic Green's function. To solve the integral equation (6), $\vec{J}_S(\vec{r}')$ (unknown surface current densities) is expanded using a set of basis functions as:

$$\vec{J}_S = \sum_{n=1}^{N} I_n \vec{f}_n. \quad (6a)$$

In this work, the Rao-Wilton-Glisson (RWG) [17] functions associated with the common edge $\overrightarrow{12}$ of the triangle pair shown in Fig. 2 were chosen as the basis functions which are expressed as:

$$\vec{f}_n = \hat{n} \times (\lambda_1 \nabla\lambda_2 - \lambda_2 \nabla\lambda_1). \quad (6b)$$

A graphical representation of RWG basis functions is reproduced from [16] in Fig. 2. Interested readers may refer to [13,16,17] for the nomenclature of symbols used and further details on the integral equation. Application of Galerkin's procedure [13-16] with same basis and weighting functions transforms the surface integral Equation (6) into a system of linear equation of the form [12-16]:

$$[Z]\{x\} = \{b\}, \quad (7)$$

where $\{x\}$ is the unknown surface current density, $\{b\}$ is the excitation vector and $[Z]$ is the coupling matrix. The mn^{th} element of $[Z]$ is given by [14,16]:

$$Z_{mn} = -j\frac{\omega\mu}{4\pi}\sum_{p=0}^{P}\sum_{q=-p}^{p}\left(\vec{f}_{pq}^{\,m}\right)^{*}.\vec{g}_{pq}^{\,n}, \quad (8)$$

where

$$\begin{Bmatrix} \vec{f}_{pq}^{\,m} \\ \vec{g}_{pq}^{\,n} \end{Bmatrix} = \oiint \begin{Bmatrix} \vec{\bar{f}}_m(\theta,\phi) \\ \vec{\bar{g}}_m(\theta,\phi) \end{Bmatrix} Y_{pq}^{*}(\theta,\phi)d\hat{k}^2, \quad (9)$$

$\vec{\bar{f}}_m$ and $\vec{\bar{g}}_m$ are the $\hat{k}$-space basis and weighting functions respectively and Y_{pq} are the orthonormalized spherical harmonics. In the above equations X^* represents the complex conjugate of X. The coupling matrix $[Z]$ is fully populated and system of linear Equation (7) becomes computationally complex for electrically large problems. A use of numerical acceleration techniques (e.g., MLFMM) can reduce the computational complexity of Equation (7) from $O(N^3)$ for traditional MoM down to $\mathrm{O(N^{1.5}\log N)}$ for single level FMM and $\mathrm{O(N\log N)}$ for MLFMM [13,19]. Moreover, as reported in [14,16] the abovementioned spherical harmonics expansion based multilevel fast multipole method (SE-MLFMM) accelerated solution of Equation (7) provides considerable amount of memory saving without compromising accuracy and the numerical speed.

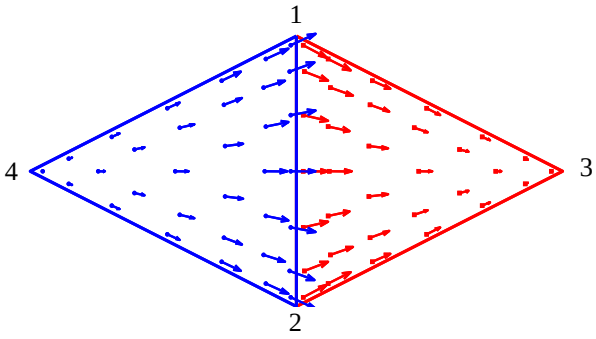

Fig. 2. WG vector basis/weighting functions for domain discretization of the electric field integral Equation (6).

In the multilevel fast multipole algorithm, the domain under consideration is enclosed in a large box, which is divided into eight smaller boxes. Each sub-box is then recursively subdivided into further smaller boxes until the side length of the smallest box is around one-half wavelength [13]. The interaction among the transmitting and receiving basis vectors residing in same or nearby smallest boxes is computed using conventional MoM. However, coupling contribution among those vectors residing in far apart boxes is calculated using MLFMM. During MLFMM, the fields radiated by different basis functions (shown with solid black arrows in the boxes on the right side of Fig. 3) within a box are first 'aggregated' into a single center. This box center then acts as the radiation center. The contribution of all radiation centers is recursively aggregated to another radiation center at the higher level. These radiated fields are then received firstly by the centers of the other boxes and then redistributed to the weighting functions (shown

with solid black arrows in the boxes on the left side of Fig. 3) belonging to the same box –so called 'disaggregation' process. Figure 3 demonstrates MLFMM process in a pictorial form. For more details on the numerical solution to EFIE, interested readers may refer to [13-19].

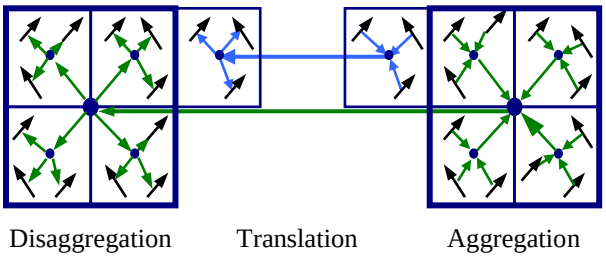

Fig. 3. Pictorial overview of MLFMM.

IV. RESULTS AND DISCUSSION

The EM solver software realized through this research was used to predict the RF performance of a Ku band ring-focus antenna system with main and sub-reflector diameters of 760 mm and 110 mm respectively. Two foci of elliptical subreflector were located at $F_{S1}(x = 0, z = 226.6)$ mm and $F_{S2}(x = 55, z = 280)$ mm in accordance with Fig. 1. A corrugated feed horn was used to illuminate the subreflector with -18 dB edge taper. GiD was used to obtain the planer triangular surface mesh of the whole structure including feed horn and subreflector supports. On average the linear dimensions of the triangular domain were of the order of λ/8 which generated around 1.4 million unknowns. The resulting matrix-vector product took around 3 hours and 40 minutes on a HP Z800 Intel® Zeon® X5690 @ 3.47 GHz dual processor with 32 GB of RAM to converge to a residual error of 8×10^{-4} which is extensively faster in comparison to general purpose commercially available 3D EM solvers.

EM solver predicted results are shown in Fig. 4 at an operating frequency of 13.75 GHz. These numerically computed results took into account the feed interaction and strut losses. A peak directivity of 38.1 dBi, around -12 dB down sidelobes and slant plane on-axis XPD better than 50 dB were predicted by our EM solver as listed in Table 1.

A prototype model of the designed ring focus antenna was manufactured and measurement results are compared with EM solver predictions in Fig. 5, where the developed reflector antenna can be seen in the inset. The measured results are in excellent agreement with EM solver predicted results in the main lobe and up to around 20 dB below the peak value. A close agreement between simulated and measured performance parameters of interest is evident from Table 1. Particularly in sidelobe regions the disagreement in predicted and measured results is mainly due to a big metallic antenna support structure used to hold the antenna on the test positioner in the anechoic chamber. This structure was not modelled in the EM solver.

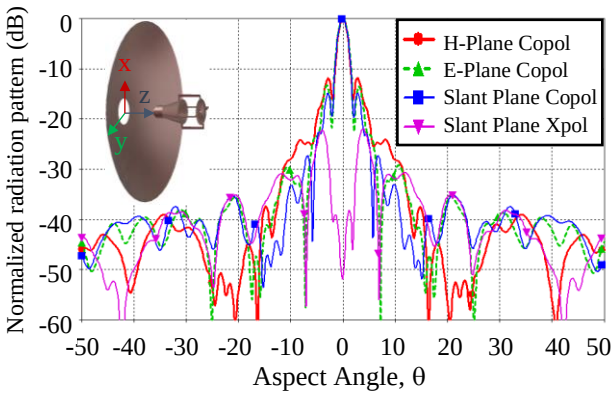

Fig. 4. Predicted performance of a 35 wavelength aperture diameter ring focus reflector antenna.

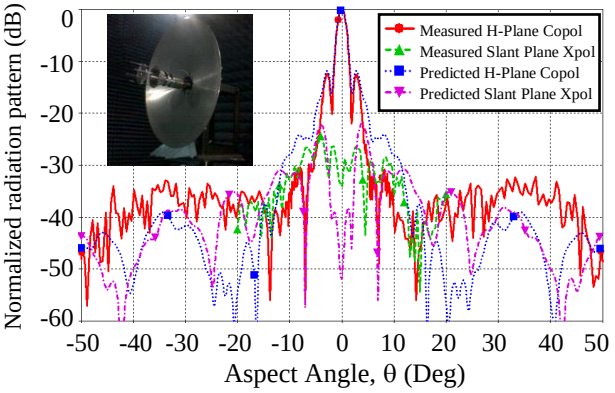

Fig. 5. Comparison of simulated and measured radiation patterns of the ring focus reflector. Inset shows the developed ring focus reflector antenna under test in an anechoic chamber.

Table 1: Summary of simulated vs. measured performance parameters

Parameter	Simulated Value	Measured Value
Peak gain	38.1 dBi	37.9 dBi
1st Sidelobe level	- 12.1 dB	- 12.6 dB
Slant plane on-axis XPD	- 50 dB	< - 30 dB

Additionally, during measurement process this metallic support structure was not covered with absorbers which resulted in higher far sidelobe levels. The difference in predicted and measured cross polarization levels is mainly due to the measurement accuracy of the anechoic chamber. It is also worth mentioning here that the feed horn used in this research was a multimode feed horn supporting TE_{11} and TE_{21} modes for communication and tracking respectively.

There was also a coupling of TE_{21} degenerate modes observed in the feed assembly design which further lowered the cross polarization. Measurements using a pure mode feed horn provided a better XPD of around 35 dB.

The equivalent surface current densities $\vec{J}_S$ on the ring-focus subreflector as well as on an exemplary Cassegrain subreflector were computed using the method described in Section III. Resulting current densities in both cases are shown in Fig. 6. For Cassegrain subreflector the central region exhibits higher amplitudes of the equivalent surface current density. In contrast, in the central region of a ring-focus subreflector very weak amplitudes of current density are observed. Weak surface current density in the central region of a ring focus subreflector may be attributed to the apex geometry along the axis.

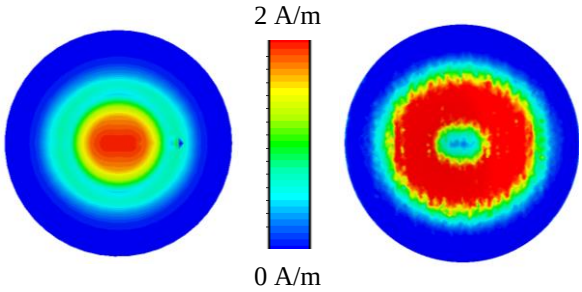

Fig. 6. Numerically computed surface current densities on Cassegrain and ring focus sub-reflectors.

It is to note that intense current densities in the central regions of a Cassegrain subreflector cause radiations towards the feed horn. These reflected radiations in the feed horn can degrade its reflection performance therefore, resulting in an overall gain degradation.

It was found through numerical simulations as well as measurements that a hole in the center of a ring focus subreflector has no significant impact on the overall antenna performance. This distinctive attribute of weak surface current density in the central region of a ring focus subreflector can be exploited to cancel radiations in certain directions e.g. to reduce the antenna sidelobe levels [21]. The inactive part of a subreflector can be removed and replaced by a dielectric lens antenna with a hyperbolic profile such that the waves passing through the lens antenna become 180˚ out of phase with those reflected by the main reflector in that particular direction.

V. CONCLUSION

A new formulation for the design of a ring-focus reflector antenna based on conic section definitions was conceived through research presented in this paper. This enabled a significant design insight and a direct CAD model creation using GiD. A fast EM solver package was developed through this research based on SE-MLFMM accelerated MoM solution of the electric field integral equation. The developed EM solver was validated through a comparison with measurements of a 35λ ring focus antenna. The distinctive feature of a ring focus sub reflector's surface current density was investigated. This will open new research areas for antenna radiation cancellation in certain directions.

ACKNOWLEDGMENT

Authors are grateful to International Center for Numerical Methods in Engineering (CIMNE) [11] for providing free license of GiD software ver. 12 which was used for domain discretization and surface current visualization.

REFERENCES

[1] A. Prata, Jr., F. J. S. Moreira, and L. R. Amaro, "Displaced-axis-ellipse reflector antenna for space-craft communications," *Microwave and Opto-electronics Conference*, vol. 1, pp. 391-395, 2003.

[2] C. A. Balanis, *Antenna Theory Analysis and Design*. New York, John Wiley & Sons, 1982.

[3] I. M. Davis, J. S. Kot, C. Granet, G. Pope, and K. Verran, "Compact shaped dual-reflector system for military Ka-band SATCOM on the move," *Proc. EuCAP2011*, pp. 3518-3521, Apr. 2011.

[4] C. Kumar, V. V. Srinivasan, V. K. Lakshmeesha, and S. Pal, "Performance of an electrically small aperture, axially displaced ellipse reflector antenna," *IEEE Antennas and Wireless Propagation Letters*, vol. 8, pp. 903-904, 2009.

[5] A. P. Popov and T. Milligan, "Amplitude aperture-distribution control in displaced axis two reflector antennas," *IEEE Antennas and Propagation Magazine*, 39, pp. 58-63, 6, Dec. 1997.

[6] F. J. S. Moreira, "Design and rigorous analysis of generalized axially symmetric dual reflector antennas," Ph.D. dissertation, *Univ. of Southern California*, Los Angeles, CA, Aug. 1997.

[7] E. G. Geterud, J. Yang, T. Ostling, and P. Bergmark, "Design and optimization of a compact wideband hat-fed reflector antenna for satellite communications," *IEEE Transactions on Antennas and Propagation*, vol. 61, pp. 125-133, 2013.

[8] A. Motevasselian and T. Ostling, "A self-supported hat-fed reflector antenna for 60 GHz frequency band," in *9th European Conference on Antennas and Propagation (EuCAP)*, pp. 1-4, 2015.

[9] F. J. S. Moreira and A. Prata, Jr., "Generalized classical axially symmetric dual-reflector antennas," *IEEE Transactions on Antennas and Propagation*, vol. 49, no. 4, pp. 547-554, Apr. 2001.

[10] C. Granet, "A simple procedure for the design of

classical displaced-axis dual reflector antennas using a set of geometric parameters," *IEEE Antennas Propag. Mag.*, vol. 41, pp. 64-72, Dec. 1999.

[11] International Center for Numerical Methods in Engineering (CIMNE). http://www.gidhome.com/

[12] R. F.Harrington, *Time Harmonis Electromagnetic Fields*. New York: McGraw-Hill, 1961.

[13] W. C. Chew, J. M. Jin, and E. Michielssen, *Fast and Efficient Algorithms in Computational Electromagnetics*. Boston: Artech House, 2001.

[14] T. F. Eibert, "A diagonalizied multilevel fast multipole method with spherical harmonics expansion of the k-space integrals," *IEEE Trans. Antenna Propagat.*, vol. 53, no. 2, pp. 814-817, Feb. 2005.

[15] A. Tzoulis and T. F. Eibert, "A hybrib FEBI-MLFMM-UTD method for numerical solutions of electromagnetic problems including arbitrarily shaped and electrically large objects," *IEEE Trans. Antenna Propagat.*, vol. 53, pp. 3358-3366, Oct. 2005.

[16] Ismatullah and T. F. Eibert, "Surface integral equation solutions by hierarchical vector basis functions and spherical harmonics based multilevel fast multipole method," *IEEE Trans. Antenna Propagat.*, vol. 57, no. 7, pp. 2084-2093, July 2009.

[17] S. M. Rao, D. R. Wilton, and A. W. Glisson, "Electromagnetic scattering by surfaces of arbitrary shape," *IEEE Trans. Antennas Propagat.*, vol. 30, no. 3, pp. 409-418, May 1982.

[18] R. Coifman, V. Rokhlin, and S. Wandzura, "The fast multipole mathod: A pedestrian prescription," *IEEE Antenna and Propagation Magazine*, vol. 35, pp. 7-12, 1993.

[19] J. M. Song and W. C. Chew, "Multilevel fast multipole algorithim for solving combined field integral equations of electromagnetic scattering," *Microwave Opt. Technology Letters*, vol. 10, no. 1, pp. 14-19, Sep. 1995.

[20] T. Wan, R. Chen, X. Hu, Y. Chen, and Y. Sheng, "Efficient direct solution of EFIE for electrically large scattering problems using H-LDLT and PE basis function," *ACES Journal*, vol. 26, no. 7, pp. 561-571, July 2011.

[21] S. Karimkashi and J. Rashed-Mohassel, "Sidelobe reduction in symmetric dual-reflector antennas using a small lens antenna," *Intl. Symp. of Microwave, Antenna, Propagation and EMC Technologies for Wireless Communications*, pp. 703-705, Aug. 2007.

Ismatullah received M.Sc. in Physics from the University of the Punjab, Lahore, Pakistan in 1999 and Dr.-Ing. from Technische Universität München,Munich, Germany in 2010. He is employed as a Scientist in SUPARCO. Together with Prof. T. F. Eibert he also received the "Best Antennas Paper Prize" of the EuCAP'2007 Conference. Numerical techniques in computational electromagnetics, antenna design, analysis and measurement are his major areas of interest.

Ghulam Ahmad is currently working towards his Ph.D. degree in mm-Wave High Gain Smart Antennas at Surrey Space Center, University of Surrey. He is the recipient of SSC-NPL mm-Waves Research Grant. In the past he was working as Communication Satellite Payload Engineer at the National Space Agency of Pakistan for more than a decade where he held various technical and management roles including Antenna Design Engineer, Antenna System Engineer, Payload System Engineer, and Deputy Project Manager. Ahmad is interested in electromagnetic theory, EM modelling, numerical techniques, antennas, antenna arrays, satellite antennas, satellites payloads, flight hardware qualification, and teaching.

Shafaat A.K.M. Ali received his M.Sc. degree from Delft University of Technology, Netherlands in 2007 and presently pursuing his Ph.D. from NED University of Engineering & Technology, Pakistan in the field of 'Metamaterial and Meta-surface Antenna'.

He joined SUPARCO (National Space Agency of Pakistan) in 2003 and is presently leading the 'Antenna & Passive Microwave' Research Laboratory. He is responsible for the design, development and testing of space borne and airborne antenna. He is also in charge of the Anechoic Chamber Test Facility. His current research work includes characterization of synthetic polymers that can be used as a meta-surface.